

Aspects of the normal state phase of copper oxide planes in high Tc superconductors.

B.C. den Hertog and M.P. Das

Department of Theoretical Physics,

Research School of Physical Sciences and Engineering,

The Australian National University, 0200 Australia.

PACS Numbers: 74.25.Jb, 74.25.Kc, 71.27.+a

Abstract

We examine various aspects of the normal state phase of CuO_2 planes in the high Tc superconductors. In particular, within the context of the three band Hubbard model, we study as a function of doping the competition between a charge density wave phase induced by oxygen breathing modes, antiferromagnetic order and paramagnetism. To account for the strong electronic interactions, we use the finite U slave boson method of Kotliar and Ruckenstein.

I. INTRODUCTION

Since the discovery of high temperature superconductivity in the cuprates, there has been a tremendous effort to deduce the properties of strongly interacting fermion systems in two-dimensions (2D). Regarding the copper oxide planes, this has led to a strong focus on purely electronic versions of the one and three band Hubbard models and their variants. Whilst this has led to progress in understanding the insulating

behaviour of the high T_c materials at half filling (as charge transfer insulators in the three band case and as Mott-Hubbard insulators in the one band case), there is little consensus as to whether superconductivity exists in either of these models or whether they are Fermi liquids or something more exotic. Furthermore, there have been relatively few attempts to understand the role of the underlying lattice in these systems. The motivation to study this last point becomes more acute with the realization that there is strong experimental evidence to suggest that a coupling does exist between charge carriers and the lattice in these materials¹⁻⁶.

From a theoretical viewpoint there have been several studies of both the one and three band Peierls Hubbard models in 2D. Here, we present a brief account of some recent results in this area. Dobry et al.⁷ suggest using exact diagonalisation of a twelve site Cu_4O_8 cluster, that in the stoichiometric state (zero doping), for any reasonable coupling of the fermions to the in-plane oxygen breathing modes and in the adiabatic limit, the system is stable against a lattice deformation. They also show that doping with one hole can produce an extended charge density wave (CDW) below a critical coupling to the lattice, and a self trapped polaron which forms a more generalised Zhang-Rice singlet above the critical coupling. On the other hand, in their Hartree Fock analysis of a system of 6×6 CuO_2 unit cells, Yonemitsu et al.^{8,9} show that in the zero doped state the CuO_2 planes can, above a critical coupling strength, undergo some type of lattice deformation, ie bond order wave, CDW. Slave boson studies of the one band Peierls Hubbard model^{10,11} show that at half filling a stable paramagnetic phase with an on-site frozen breathing mode induced long range CDW occurs below a critical value of the Hubbard repulsion U . Mitra and Behera show¹² that in general electron correlation suppresses the CDW state.

The purpose of this paper is to examine systematically as a function of doping the stability of the three band Hubbard model¹⁶⁻¹⁹ against a lattice deformation created

by the in-plane oxygen breathing modes. More to the point, we wish to study whether this model is susceptible to at least a paramagnetic CDW phase either at zero or finite doping, and more importantly, whether the copper oxide planes can develop from a homogenous antiferromagnetic phase in the undoped system to a paramagnetic CDW phase at finite doping.

Using the slave boson method of Kotliar and Ruckenstein (KR)¹³, we are able to take into account the strong on-site and nearest neighbour fermion interactions. This finite Hubbard U technique has the advantage of being able to cope with the strong coupling regime in a non-perturbative way, and at the same time it is in reasonable agreement with Monte Carlo results¹⁵ even at the mean field level. Thus, armed with this apparatus, we are able to examine as a function of doping and interaction parameters at the mean field level, the competition between an undistorted antiferromagnetic state, the normal paramagnetic state and a paramagnetic CDW state induced by lattice deformations. Lastly, because we use the three band model, we are able to accommodate a more complete tight binding band structure which includes oxygen-oxygen hopping in order to produce a realistic Fermi surface²⁰.

II. MODEL CALCULATIONS

To examine the possibility of a lattice instability, we include an electron-phonon coupling which modifies the copper-oxygen hopping strength depending on whether an oxygen ion is displaced towards a copper ion or away from it⁷⁻⁹. To simplify calculations we make the following approximations. Firstly, we assume a frozen phonon picture for the oxygen ions and thus work in the adiabatic limit. Secondly, we assume that the oxygen-oxygen hopping is not modified by the relative displacements of the oxygen ions. With these provisions, the three band Hubbard Hamiltonian with electron-phonon coupling (three band Peierls Hubbard model) is given by

$$\begin{aligned}
H = & \sum_{\langle ij \rangle \sigma} t_{ij} (c_{i\sigma}^\dagger c_{j\sigma} + h.c.) + \sum_{\langle jj' \rangle \sigma} t_{jj'} (c_{j\sigma}^\dagger c_{j'\sigma} + h.c.) + \sum_{i\sigma} \epsilon_i c_{i\sigma}^\dagger c_{i\sigma} + \sum_{j\sigma} \epsilon_j c_{j\sigma}^\dagger c_{j\sigma} \\
& + \sum_{i\sigma} U n_{i\uparrow} n_{i\downarrow} + \sum_{\langle ij \rangle \sigma \sigma'} V n_{i\sigma} n_{j\sigma'} + \sum_j \frac{1}{2} K u_j^2, \tag{1}
\end{aligned}$$

where $c_{i\sigma}^\dagger$ creates a hole at a copper site i with spin σ and $c_{j\sigma}^\dagger$ creates a hole at an oxygen site j with spin σ . The on-site copper (oxygen) energy is given by ϵ_i (ϵ_j). The hopping between copper and oxygen sites is represented by t_{ij} and its sign depends on the symmetry of the copper $d_{x^2-y^2}$ and oxygen p_x and p_y orbitals. The sum over $\langle ij \rangle$ refers to nearest neighbour copper and oxygen sites only. Without lattice deformation and in the nearest neighbour hopping picture, t_{ij} would be given by a constant t . However, t_{ij} is assumed to be modified by the in-plane breathing modes as stated above in the following manner^{8,9}. If the surrounding oxygen sites are deformed towards a copper site, then $t_{ij} = t + \alpha u_j$, where u_j is the absolute value of the oxygen lattice displacement from its mean position. Similarly, if the surrounding oxygens are displaced away from a copper site, then the hopping becomes $t_{ij} = t - \alpha u_j$. The parameter $t_{jj'}$ in (1) represents oxygen-oxygen hopping and its sign also depends on the symmetry of the oxygen orbitals. The sum over $\langle jj' \rangle$ refers to hopping between pairs of second nearest neighbour oxygen j and j' sites. The U term represents the Hubbard interaction at copper sites whilst V is the nearest neighbour interaction between holes at adjacent copper and oxygen sites. We neglect an on-site interaction at the oxygen sites since the probability of double occupancy of these sites by holes for physically reasonable hopping and interaction parameters and not too large doping is quite small. The classical force constant of the oxygen ions is represented by the parameter K . Following references⁷⁻⁹ we introduce a dimensionless electron-phonon coupling constant $\lambda \equiv \alpha^2/Kt$.

To accommodate the strong on-site and nearest neighbour fermion interactions, we introduce four auxiliary bosons fields¹³ for the copper sites. In this scheme, each possible electronic configuration of the copper site is represented by one of these fields.

The fermionic creation operator is mapped $c_{i\sigma}^\dagger \mapsto q_{i\sigma} c_{i\sigma}^\dagger$ where $q_{i\sigma}$ is defined as

$$q_{i\sigma} \equiv \frac{e_i s_{i\sigma}^\dagger + s_{i\bar{\sigma}} d_i^\dagger}{\sqrt{(1 - d_i^\dagger d_i - s_{i\sigma}^\dagger s_{i\sigma})(1 - e_i^\dagger e_i - s_{i\bar{\sigma}}^\dagger s_{i\bar{\sigma}})}} . \quad (2)$$

The boson fields $e_i, s_{i\sigma}$, and d_i represent empty, single with spin σ and double occupation of copper sites respectively. The square root terms in $q_{i\sigma}$ ensures that the mapping becomes trivial at the mean field level in the non-interacting limit $U \rightarrow 0, V \rightarrow 0$. The KR slave boson method replaces the Hubbard interaction with a bilinear term involving the boson double occupancy fields whilst renormalising the hopping energy of the fermion quasiparticles by the factor $q_{i\sigma}$. Unphysical states arising from the enlarged Hilbert space are eliminated via the following constraints;

$$c_{i\sigma}^\dagger c_{i\sigma} = s_{i\sigma}^\dagger s_{i\sigma} + d_i^\dagger d_i \quad (3)$$

and

$$e_i^\dagger e_i + \sum_{\sigma} s_{i\sigma}^\dagger s_{i\sigma} + d_i^\dagger d_i - 1 = 0 , \quad (4)$$

which represent charge conservation and the completeness of the bosonic operators respectively. With this mapping in place the Hamiltonian becomes;

$$\begin{aligned} H = & \sum_{\langle ij \rangle \sigma} t_{ij} (q_{i\sigma} c_{i\sigma}^\dagger c_{j\sigma} + h.c.) + \sum_{\langle jj' \rangle \sigma} t_{jj'} (c_{j\sigma}^\dagger c_{j'\sigma} + h.c.) + \sum_{i\sigma} (\epsilon_i + \gamma_{i\sigma}) c_{i\sigma}^\dagger c_{i\sigma} \\ & + \sum_{j\sigma} \epsilon_j c_{j\sigma}^\dagger c_{j\sigma} + \sum_i U d_i^\dagger d_i + \sum_{\langle ij \rangle \sigma \sigma'} V (s_{i\sigma}^\dagger s_{i\sigma} + d_i^\dagger d_i) c_{j\sigma'}^\dagger c_{j\sigma'} + \sum_j \frac{1}{2} K u_j^2 \\ & - \sum_{i\sigma} \gamma_{i\sigma} (s_{i\sigma}^\dagger s_{i\sigma} + d_i^\dagger d_i) + \sum_i \gamma'_i (e_i^\dagger e_i + \sum_{\sigma} s_{i\sigma}^\dagger s_{i\sigma} + d_i^\dagger d_i - 1) , \end{aligned} \quad (5)$$

where $\gamma_{i\sigma}$ and γ'_i are Lagrange multipliers enforcing the constraints on the boson fields.

The partition function for the system can be expressed as a functional integral over complex (bosons) and Grassmann fields (fermions). Integrating exactly over the Grassmann fields leaves the partition function as¹⁴;

$$Z = \int D[e] D[s_\sigma] D[d] D[\gamma] D[\gamma'] e^{-S_{eff}^{boson}} , \quad (6)$$

where the bosonic action is

$$\begin{aligned}
S_{eff}^{boson} = \int_0^\beta d\tau \left\{ \text{Tr} \ln \left[t_{ij} q_{i\sigma} + (\gamma_{i\sigma} + \epsilon_i + \partial_\tau) \delta_{ji} \right. \right. \\
+ \left. \left. \left(\epsilon_j + \partial_\tau + V \sum_{nn\sigma'} (s_{nn\sigma'}^\dagger s_{nn\sigma'} + d_{nn}^\dagger d_{nn}) \right) \delta_{ij} + t_{jj'} \delta_{ij'} \right] \right. \\
+ \sum_{i\sigma} s_{i\sigma}^\dagger (\gamma'_i + \partial_\tau - \gamma_{i\sigma}) s_{i\sigma} + \sum_{i\sigma} d_i^\dagger (U + \gamma'_i + \partial_\tau - \gamma_{i\sigma}) d_i \\
\left. + \sum_i e_i^\dagger (\gamma'_i + \partial_\tau) e_i - \sum_i \gamma'_i + \sum_j \frac{1}{2} K u_j^2 \right\} \quad (7)
\end{aligned}$$

and the subscript nn implies nearest neighbour summations only.

To evaluate the partition function we employ the saddle point approximation¹³ where all the boson fields are c numbers. Accordingly, at $T = 0$ the energy per cell is given by

$$\begin{aligned}
E = \frac{1}{N} \sum_{\langle ij \rangle \sigma} q_{i\sigma} t_{ij} \langle c_{i\sigma}^\dagger c_{j\sigma} + h.c. \rangle + \frac{1}{N} \sum_{\langle jj' \rangle \sigma} t_{jj'} \langle c_{j\sigma}^\dagger c_{j'\sigma} + h.c. \rangle \\
+ \frac{1}{N} \sum_{i\sigma} (\epsilon_i + \gamma_{i\sigma}) n_{i\sigma} + \frac{1}{N} \sum_{j\sigma} \epsilon_j n_{j\sigma} \\
+ \frac{1}{N} \sum_i U d_i^2 + \frac{1}{N} \sum_{\langle ij \rangle \sigma \sigma'} V (s_{i\sigma}^2 + d_i^2) n_{j\sigma'} + \frac{1}{N} \sum_j \frac{1}{2} K u_j^2 \\
- \frac{1}{N} \sum_{i\sigma} \gamma_{i\sigma} (s_{i\sigma}^2 + d_i^2) + \frac{1}{N} \sum_i \gamma'_i (e_i^2 + \sum_\sigma s_{i\sigma}^2 + d_i^2 - 1) , \quad (8)
\end{aligned}$$

where N is the number of unit cells.

Equation (8) must be minimized with respect to the boson fields. The CDW phase can be examined by dividing the copper lattice into two sub-lattices A and B, which results in a doubling of the unit cell and hence a halving of the Brillouin zone. The above energy per cell will be modified by inclusion of summations over the sub-lattices and by dividing the boson fields into e_ν, s_ν and d_ν where $\nu = A, B$. Here we have assumed a paramagnetic CDW phase, thus $s_{\nu\sigma} = s_{\nu\bar{\sigma}}$.

To examine the purely antiferromagnetic state, the copper lattice is again divided and the unit cell doubled. The displacement of the oxygen ions is set to zero. Due to the symmetry of such a phase, $s_{A\sigma} = s_{B\bar{\sigma}}$, $\gamma_{A\sigma} = \gamma_{B\bar{\sigma}}$ and $d_A = d_B$. The homogeneous

paramagnetic phase can be studied by a straight forward minimization of the above energy per cell.

A. Charge Density Wave Phase.

In this subsection we derive the self consistent minimization equations for the CDW phase. Dividing the copper lattice into an A and B sub-lattices and minimizing the energy per Cu_2O_4 cell with respect to u_j , we get

$$\frac{1}{M} \frac{\partial}{\partial u_j} \left[\sum_{\langle A_j \rangle \sigma} q_A t_A \langle c_{A\sigma}^\dagger c_{j\sigma} + h.c. \rangle + \sum_{\langle B_j \rangle \sigma} q_B t_B \langle c_{B\sigma}^\dagger c_{j\sigma} + h.c. \rangle \right] + 4K u_j = 0 \quad , \quad (9)$$

where M is the number of Cu_2O_4 cells. Moving to Bloch functions the above equation becomes;

$$2\alpha(q_A \Omega_A - q_B \Omega_B) + q_A \Lambda_A + q_B \Lambda_B + 4K u_j = 0 \quad , \quad (10)$$

where

$$\begin{aligned} \Omega_A = & \frac{1}{2M} \sum_{\mathbf{k}\sigma} \left(- \left[e^{ik_x(\frac{1}{2}-u_j)} \langle c_{A\mathbf{k}\sigma}^\dagger c_{x_1\mathbf{k}\sigma} \rangle + h.c. \right] + \left[e^{-ik_x(\frac{1}{2}-u_j)} \langle c_{A\mathbf{k}\sigma}^\dagger c_{x_2\mathbf{k}\sigma} \rangle + h.c. \right] \right. \\ & \left. + \left[e^{ik_y(\frac{1}{2}-u_j)} \langle c_{A\mathbf{k}\sigma}^\dagger c_{y_1\mathbf{k}\sigma} \rangle + h.c. \right] - \left[e^{-ik_y(\frac{1}{2}-u_j)} \langle c_{A\mathbf{k}\sigma}^\dagger c_{y_2\mathbf{k}\sigma} \rangle + h.c. \right] \right) \quad , \quad (11) \end{aligned}$$

$$\begin{aligned} \Omega_B = & \frac{1}{2M} \sum_{\mathbf{k}\sigma} \left(\left[e^{-ik_x(\frac{1}{2}+u_j)} \langle c_{B\mathbf{k}\sigma}^\dagger c_{x_1\mathbf{k}\sigma} \rangle + h.c. \right] - \left[e^{ik_x(\frac{1}{2}+u_j)} \langle c_{B\mathbf{k}\sigma}^\dagger c_{x_2\mathbf{k}\sigma} \rangle + h.c. \right] \right. \\ & \left. - \left[e^{-ik_y(\frac{1}{2}+u_j)} \langle c_{B\mathbf{k}\sigma}^\dagger c_{y_1\mathbf{k}\sigma} \rangle + h.c. \right] + \left[e^{ik_y(\frac{1}{2}+u_j)} \langle c_{B\mathbf{k}\sigma}^\dagger c_{y_2\mathbf{k}\sigma} \rangle + h.c. \right] \right) \quad , \quad (12) \end{aligned}$$

$$\begin{aligned} \Lambda_A = & \frac{t_A}{M} \sum_{\mathbf{k}\sigma} \left(- \left[-ik_x e^{ik_x(\frac{1}{2}-u_j)} \langle c_{A\mathbf{k}\sigma}^\dagger c_{x_1\mathbf{k}\sigma} \rangle + h.c. \right] + \left[ik_x e^{-ik_x(\frac{1}{2}-u_j)} \langle c_{A\mathbf{k}\sigma}^\dagger c_{x_2\mathbf{k}\sigma} \rangle + h.c. \right] \right. \\ & \left. + \left[-ik_y e^{ik_y(\frac{1}{2}-u_j)} \langle c_{A\mathbf{k}\sigma}^\dagger c_{y_1\mathbf{k}\sigma} \rangle + h.c. \right] - \left[ik_y e^{-ik_y(\frac{1}{2}-u_j)} \langle c_{A\mathbf{k}\sigma}^\dagger c_{y_2\mathbf{k}\sigma} \rangle + h.c. \right] \right) \quad (13) \end{aligned}$$

and

$$\begin{aligned} \Lambda_B = & \frac{t_B}{M} \sum_{\mathbf{k}\sigma} \left(\left[-ik_x e^{-ik_x(\frac{1}{2}+u_j)} \langle c_{B\mathbf{k}\sigma}^\dagger c_{x_1\mathbf{k}\sigma} \rangle + h.c. \right] - \left[ik_x e^{ik_x(\frac{1}{2}+u_j)} \langle c_{B\mathbf{k}\sigma}^\dagger c_{x_2\mathbf{k}\sigma} \rangle + h.c. \right] \right. \\ & \left. - \left[-ik_y e^{-ik_y(\frac{1}{2}+u_j)} \langle c_{B\mathbf{k}\sigma}^\dagger c_{y_1\mathbf{k}\sigma} \rangle + h.c. \right] + \left[ik_y e^{ik_y(\frac{1}{2}+u_j)} \langle c_{B\mathbf{k}\sigma}^\dagger c_{y_2\mathbf{k}\sigma} \rangle + h.c. \right] \right) \quad . \quad (14) \end{aligned}$$

The hopping parameters are defined by $t_A = t + \alpha u_j$ and $t_B = t - \alpha u_j$. That is to say that the oxygen ions are breathed in towards the copper A sites thus strengthening the hopping between them, and breathed out from the copper B sites weakening the hopping between B sites and oxygen sites. The lattice displacement variable is in units of the Cu-Cu lattice spacing. The oxygen sites are labeled around a copper A site in the following way. Looking down upon the CuO_2 plane, x_1 is the oxygen site to the right of the A site, x_2 is to the left, y_1 is above and y_2 is below.

Minimizing equation (8) with respect to the boson fields on the A and B sub-lattices, we obtain the following equations;

$$t_\nu \Omega_\nu \frac{\partial q_\nu}{\partial d_\nu} + U d_\nu + 8V n_j d_\nu - 2\gamma_\nu d_\nu + d_\nu \gamma'_\nu = 0 \quad , \quad (15)$$

$$t_\nu \Omega_\nu \frac{\partial q_\nu}{\partial s_\nu} + 8V n_j s_\nu - 2\gamma_\nu s_\nu + 2\gamma'_\nu s_\nu = 0 \quad (16)$$

and

$$t_\nu \Omega_\nu \frac{\partial q_\nu}{\partial e_\nu} + \gamma'_\nu e_\nu = 0 \quad , \quad (17)$$

where $\nu = A, B$. Combining these equations with the constraints we arrive at the minimization equations for the A and B sub-lattices;

$$U = \frac{t_\nu \Omega_\nu}{\sqrt{\frac{n_\nu}{2}(1 - \frac{n_\nu}{2})}} \left[\frac{1 + 2d_\nu^2 - \frac{3n_\nu}{2}}{\sqrt{(1 + d_\nu^2 - n_\nu)(\frac{n_\nu}{2} - d_\nu^2)}} + \frac{2d_\nu^2 - \frac{n_\nu}{2}}{\sqrt{d_\nu^2(\frac{n_\nu}{2} - d_\nu^2)}} \right] \quad . \quad (18)$$

The total energy per cell is thus minimized by self consistently diagonalizing the fermion part of the effective Hamiltonian in order to calculate $n_\nu, \Omega_\nu, \Lambda_\nu$, and u_j and solving equations (10) and (18).

In presenting results for this phase, we begin by studying the interplay between Coulomb interaction and electron-phonon coupling in the undoped state. We have used the parameter set²¹ of $t = 1.3$, $t_{jj'} = 0.65$, $V = 1.2$, and $\epsilon_j - \epsilon_i = 3.6$ where all energies are in eV. The force constant $K = 32t \text{ eV}/\text{\AA}^8$. This parameter set is used

for all calculations. Of course the overall stability of the paramagnetic CDW phase can only be considered after comparing the total energy to that of the homogenous paramagnetic and antiferromagnetic phases, which we will consider in later sections.

Fig. 1 shows the charge density difference between copper A and B sites as a function of U for different electron phonon coupling strengths. In this CDW phase, the electron phonon coupling has increased the copper A site charge density due to the increased hopping amplitude t_A . Conversely, the charge density at the B sites has been decreased significantly due to t_B . This process is hindered by the Hubbard repulsion at the copper sites, which naturally works against this increased charge density at the A sites. The results of Fig. 1 seem to indicate that at a certain value of U , for a given λ , the system undergoes a first order transition to the homogenous paramagnetic state. At this point the Coulomb repulsion has become too strong to sustain the CDW. As U is increased from zero the A site charge density decreases, however the B site charge density does not increase at the same rate. There is an overall shift in charge to the oxygen sites as U is increased. This increase is shown in Fig. 2. The charge continues to build up on the oxygen sites until just before U_{crit} , where there is a small reversal in charge flow. It can also be seen in Fig. 1 that the stability of the system as a function of U is quite sensitive to the electron-phonon coupling strength. Fig. 1 shows that for a reasonably strong coupling ($\lambda > 0.8$) the system is quite robust (at least there is a local minimum in the energy) for any physically reasonable value of U for the CuO_2 planes.

In Fig. 3 we show the difference in the charge densities on copper A and B sites Δ ($\equiv n_A - n_B$) as a function of doping ($\delta \equiv n - 1$) for the parameter sets $\lambda = 1.00$, $U = 10$ eV and $\lambda = 0.95$, $U = 6$ eV. There is an almost linear decrease in the CDW order parameter as the system is doped until one reaches $\delta_{crit} \approx 0.49$ for both parameter sets. Prior to δ_{crit} , the B site charge is almost localised due to an extremely

small effective hopping $q_B t_B \sim 0.1$. The double occupancy on the B sites is such that $d_B^2 \sim 10^{-4}$, and remains at this magnitude as more charge builds up on the B sites as the system is doped. Because of this, the holes on the B sites become more and more localised as extra holes are added to the systems since $q_B \rightarrow 0$ as $n_B \rightarrow 1$ and $d_B \rightarrow 0$ ²². As $\delta \rightarrow \delta_{crit}$, $n_B \rightarrow 1$, thus when δ exceeds δ_{crit} and therefore $n_B > 1$ the system is required to obey the physical constraint $d_B^2 > n_B - 1$, causing a finite Hubbard energy on the B sites which makes the system in this phase unstable.

B. Antiferromagnetic Phase.

There have been previous slave boson calculations carried out on the antiferromagnetic and paramagnetic phases of the three band Hubbard model by Zhang et al²³. However, they have used a parameter set containing a small oxygen-oxygen hopping parameter ($t_{jj'} = 0.2$ eV) and charge transfer energy ($\epsilon_j - \epsilon_i = 1.5$ eV). Also, their value of U (6 eV), is just at the lower bound of what is a reasonable value for the Hubbard interaction on copper sites in the copper oxide planes²⁴. This being the case, it is useful to redo and expand on some of these types of calculations with improved estimates of the hopping and interaction parameters, especially when comparing the energies of these phases to a phonon driven one.

The saddle point equations in the antiferromagnetic phase are derived by again dividing the copper lattice into A and B sub-lattices. As stated before, the symmetry of this phase implies $e_A = e_B$, $s_{A\uparrow} = s_{B\downarrow} \equiv s_\uparrow$, $s_{A\downarrow} = s_{B\uparrow} \equiv s_\downarrow$ and $d_A = d_B \equiv d$. Following a procedure similar to that in the CDW section, the following minimization equation is derived;

$$U = \frac{\Omega_\uparrow t}{\sqrt{(1 - n_{i\uparrow})n_{i\uparrow}}} \left[\frac{1 + 2d^2 - n_i - n_{i\uparrow}}{\sqrt{(1 + d^2 - n_i)(n_{i\uparrow} - d^2)}} + \frac{2d^2 - n_{i\downarrow}}{\sqrt{d^2(n_{i\downarrow} - d^2)}} \right]$$

$$+ \frac{\Omega_{\downarrow} t}{\sqrt{(1 - n_{i\downarrow})n_{i\downarrow}}} \left[\frac{1 + 2d^2 - n_i - n_{i\downarrow}}{\sqrt{(1 + d^2 - n_i)(n_{i\downarrow} - d^2)}} + \frac{2d^2 - n_{i\uparrow}}{\sqrt{d^2(n_{i\uparrow} - d^2)}} \right] , \quad (19)$$

where

$$\Omega_{\uparrow} \equiv \frac{1}{2M} \sum_{\langle Aj \rangle} (\langle c_{A\uparrow}^{\dagger} c_{j\uparrow} \rangle + h.c.) = \frac{1}{2M} \sum_{\langle Bj \rangle} (\langle c_{B\downarrow}^{\dagger} c_{j\downarrow} \rangle + h.c.) ,$$

$$\Omega_{\downarrow} \equiv \frac{1}{2M} \sum_{\langle Aj \rangle} (\langle c_{A\downarrow}^{\dagger} c_{j\downarrow} \rangle + h.c.) = \frac{1}{2M} \sum_{\langle Bj \rangle} (\langle c_{B\uparrow}^{\dagger} c_{j\uparrow} \rangle + h.c.) ,$$

and $n_i \equiv n_A = n_B$, $n_{i\uparrow} \equiv n_{A\uparrow} = n_{B\downarrow}$ and $n_{i\downarrow} \equiv n_{A\downarrow} = n_{B\uparrow}$. Equation (19) is solved self consistently with the diagonalized one body fermion Hamiltonian in order to minimize the energy per magnetic cell.

Fig. 4 shows the quasiparticle band structure in the antiferromagnetic phase at zero doping using the reference parameter set and $U = 10$ eV. The coordinates in the figure represent the non-magnetic Brillouin zone. One can clearly see the lower and upper Hubbard bands and the dispersion of the oxygen bands in between. The lower Hubbard band is fully occupied at this hole concentration and consists of mainly (73%) of copper states. Doped holes go mainly to the oxygen sites and occupy states around the $(\pi/2, \pi/2)$ region (the magnetic Brillouin zone). It is interesting to compare this figure with the Hartree Fock band structure obtained by Yonemitsu et al.⁹. Although their parameter set is slightly different (in units of eV; $t = 1, t_{jj'} = 0.5, U = 8, V = 1$ and $U_{oxygen} = 3$), the four lowest bands are similar with the same curvature and band minima. This is despite the fact that they include a Hubbard repulsion on the oxygen sites. For the same parameter set Fig. 5 shows the quasiparticle band structure for a doping of $\delta = 0.25$. It can be seen from this figure that new states have formed within the original insulating gap of the undoped system reducing the gap significantly.

In Fig. 6 we show the dependence of the staggered magnetic moment m ($\equiv n_{A\uparrow} - n_{A\downarrow}$) on U in the undoped state. As U decreases to ≈ 1.75 eV the lower and upper

Hubbard bands begin to overlap. Beyond this point our results become inaccurate as the doping can not be pinned at zero. However, as U increases from this point there is a steady increase in the staggered moment until it saturates for large U at $m \approx 0.75$. Similar qualitative behaviour is found in the one band Hubbard model using Monte Carlo techniques²⁵. As shown by Zhang *et al.*²³ the effect of $t_{jj'}$ is to decrease the magnetic moment because it becomes energetically favourable for some of the holes to move on the oxygen network rather than occupy mainly copper sites. The behaviour of the staggered moment upon doping is shown in Fig. 7 for the reference parameter set. The dotted line represents $U = 10$ eV and the solid line is $U = 6$ eV. The local Cu moment vanishes almost discontinuously at δ_{crit} indicating the likelihood of a first order phase transition. The precise point at which the transition occurs is unclear due to the extremely slow convergence near this region. It is worth noting that apparently U has little effect on the value of δ at which the antiferromagnetic order vanishes. The variation of other parameters such as hopping and charge transfer energies have a much more significant effect²³. The relatively small effect of varying U may be due to the fact that at least in the undoped state, the antiferromagnetic order parameter has already begun to saturate at $U = 6$ eV.

C. Energy per CuO₂ cell.

In Figs. 8 and 9 we show the calculated energy per CuO₂ cell as a function of doping for the CDW, antiferromagnetic and paramagnetic phases. The various energies in Fig. 8 were calculated with an electron-phonon coupling of $\lambda = 1.00$ and $U = 10$ eV. The figure clearly shows that for this parameter set the system is stable against a breathing mode induced paramagnetic CDW ground state and that as a function of doping the system moves from an antiferromagnetic state to a homogenous paramagnetic one. At this value of λ the effective hopping parameter $t_B = 0.07$. A stronger coupling drives

$t_B \rightarrow 0$ causing the copper B sites to be completely localised and thus it becomes debatable whether it is useful to do calculations in such a region. However, if one believes that one can and assumes that the energy dependence on doping for the CDW phase has the same gradient as shown in Fig. 8 then it may be possible to find a stable CDW at $\delta_{crit} > 0.4$. The same type of calculations are shown in Fig. 9 but in this case $U = 6$ eV and $\lambda = .95$. It is interesting to note that here the system starts in the antiferromagnetic phase at zero doping then moves to a paramagnetic phase at $\delta \approx 0.33$ and then to a paramagnetic CDW phase at $\delta \approx 0.4$. These calculations indicate that at least in the highly doped systems, the three band Hubbard model is susceptible at this mean field level to some sort of lattice distortion (we have shown here the paramagnetic CDW) given the appropriate interaction parameters. However we have shown that for a larger value of U and reasonably strong electron-phonon coupling, this model suppresses the CDW phase.

III. CONCLUSIONS.

Using the finite U slave boson method of KR¹³ to account for the strong fermion-fermion interactions, we have examined for different interaction parameters the possibility of an instability of the three band Hubbard model towards a paramagnetic CDW state induced by the oxygen breathing modes of the copper oxide planes. We have found that this model can at the mean field level, exhibit an instability towards such a phase at large doping given a low value of the Hubbard repulsion on copper sites $U(\approx 6$ eV). For larger U the CDW is suppressed. Also, we have examined antiferromagnetic correlations at both zero and finite doping. We have shown that like the one band Hubbard model, the three band model antiferromagnetic order parameter saturates as a function of U and the system undergoes a phase transition to the homogenous paramagnetic phase at finite doping. A suggestion for further calculation would be to

examine antiferromagnetic correlations in the CDW phase, particularly its importance at low doping.

IV. ACKNOWLEDGEMENTS

This work was initiated at the High T_c Superconductivity workshop in Canberra, Australia 1994. We thank D.C. Mattis, J.M. Wheatley and T.C. Choy for useful discussions. B.C.dH acknowledges the financial support of the Australian Federal Government in the form of an Australian Postgraduate Award Scholarship.

REFERENCES

- ¹ M. Arai, K. Yamada, Y. Hikada, S. Itoh, Z.A. Bowden, A.D. Taylor and Y. Endoh, Phys. Rev. Lett. **69**, 359 (1992).
- ² B. Freidl, C. Thomsen and M. Cardona, Phys. Rev. Lett. **65**, 915 (1990).
- ³ M.C. Krantz, C. Thomsen, Hj. Mattausch, and M. Cardona, Phys. Rev. B **50**, 1165 (1994).
- ⁴ A.P. Litvinchuk, C. Thomsen, M. Cardona, L. Börjesson, P. Berastegui and L.-G. Johnson, Phys. Rev. B **50**, 1171 (1994).
- ⁵ P. Brüesch and W. Bührer, Z. Phys. B **70**, 1 (1988).
- ⁶ P. Steiner, V. Kinsinger, I. Sander, B. Siegwart, S. Hüffner and C. Politis, Z. Phys. B **67**, 19 (1987).
- ⁷ A. Dobry, A. Greco, J. Lorenzana and J. Riera, Phys. Rev. B **49**, 505 (1994).
- ⁸ K. Yonemitsu, A.R. Bishop and J. Lorenzana, Phys. Rev. Lett. **69**, 965 (1992).
- ⁹ K. Yonemitsu, A.R. Bishop and J. Lorenzana, Phys. Rev. B **47**, 12059 (1993).
- ¹⁰ H. Feshke, M. Deeg and H. Büttner, Phys. Rev. B **46**, 3713 (1992).
- ¹¹ M. Deeg, H. Feshke and H. Büttner, Z. Phys. B **88**, 283 (1992).
- ¹² Manidipa Mitra and S.N. Behera, Condens. Matt. Mat. Commun. **1**, 247 (1994).
- ¹³ G. Kotliar and A.E. Ruckenstein, Phys. Rev. Lett. **57**, 1362 (1986).
- ¹⁴ See, for example John W. Negele and Henri Orland, *Quantum many-particle systems*, (Addison-Wesley, Redwood City, 1988).
- ¹⁵ L. Lilly, A. Maramatsu and W. Hanke, Phys. Rev. Lett. **65**, 1379 (1990).

- ¹⁶ V.J. Emery, Phys. Rev. Lett. **58**, 2794 (1987).
- ¹⁷ P.B. Littlewood, C.M. Varma and E. Abrahams, Phys. Rev. Lett. **60**, 379 (1987).
- ¹⁸ C.M. Varma, S. Schmit-Rink and E. Abrahams, Solid State Commun. **62**, 681 (1987).
- ¹⁹ V.J. Emery and G. Reiter, Phys. Rev. B **38**, 4547 (1988).
- ²⁰ M.P. López Sancho, J. Rubio, M.C. Refolio and J.M. López Sancho, Phys. Rev. B **52**, 6920 (1995).
- ²¹ M.S. Hybertson, M. Schlüter and N.E. Christensen, Phys. Rev. B **39**, 9028 (1989).
- ²² B.C. den Hertog and M.P. Das, Solid State Commun. **98**, 7 (1996). Note that in this reference there are small typographical errors in equations (3) and (12). In equation (3) the square root terms should be in the denominator. In equation (12) the derivative should be w.r.t. n_i , not d_i . None of the results are effected by these errors.
- ²³ Weiyi Zhang, M. Avignon and K.H. Bennemann, Phys. Rev. B **42**, 10192 (1990).
- ²⁴ F. Mila, Phys. Rev. B **38**, 11358 (1988).
- ²⁵ S.R. White, D.J. Scalapino, R.L. Sugar, E.Y. Loh, J.E. Gubernatis and R.T. Scalet-ter, Phys. Rev. B **40**, 506 (1989).

Figure Captions.

Fig 1: Dependence of the CDW order parameter on the Hubbard repulsion U for different electron-phonon coupling strengths and zero doping.

Fig 2: Total oxygen site occupancy for a Cu_2O_4 cell as a function of U for different electron-phonon coupling strengths at zero doping.

Fig 3: Behaviour of the CDW order parameter upon doping for different interaction parameter sets.

Fig 4: Antiferromagnetic band structure for zero doping and $U = 10$ eV. The lowest band is fully occupied whilst the remaining bands are empty.

Fig 5: Antiferromagnetic bandstructure at a doping of $\delta = 0.25$ and $U = 10$ eV. The original gap has narrowed and the second lowest band is partially filled.

Fig 6: Behaviour of the staggered moment on Cu sites in the antiferromagnetic phase as a function of U at zero doping.

Fig 7: Doping dependence of the staggered moment for different values of U .

Fig 8: Energy per CuO_2 cell as a function of doping for the various phases. Here $U = 10$ eV and $\lambda = 1.00$.

Fig 9: Same as Fig. 8 but here the interaction parameters are $U = 6$ eV and $\lambda = 0.95$.

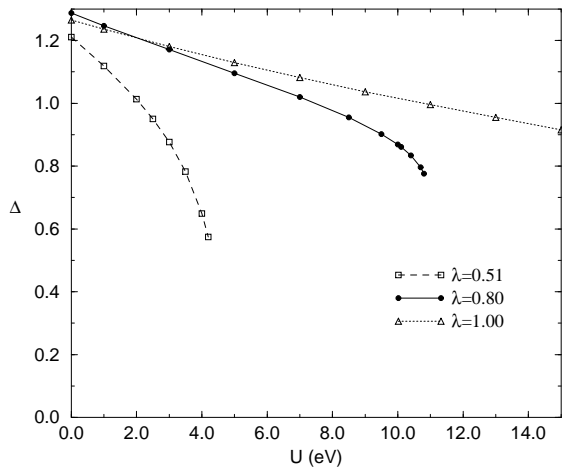


Figure 1

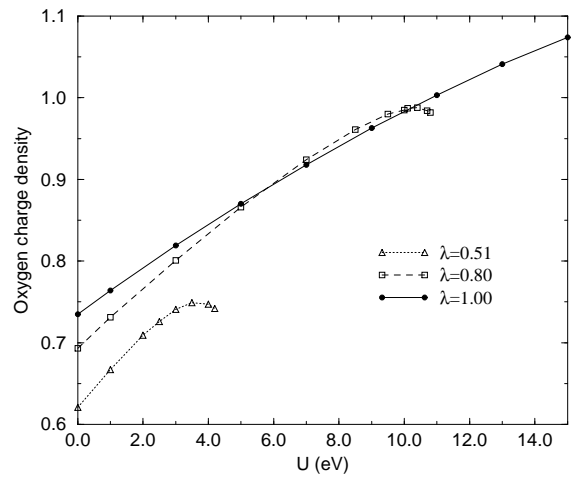


Figure 2

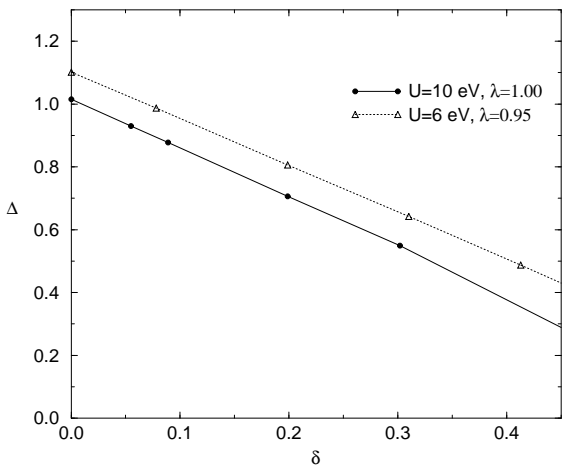


Figure 3

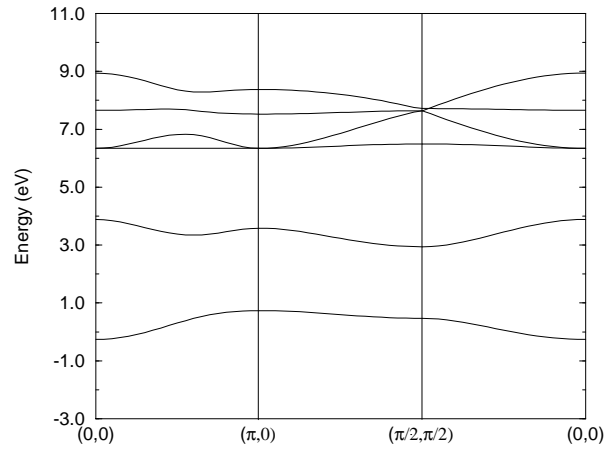


Figure 4

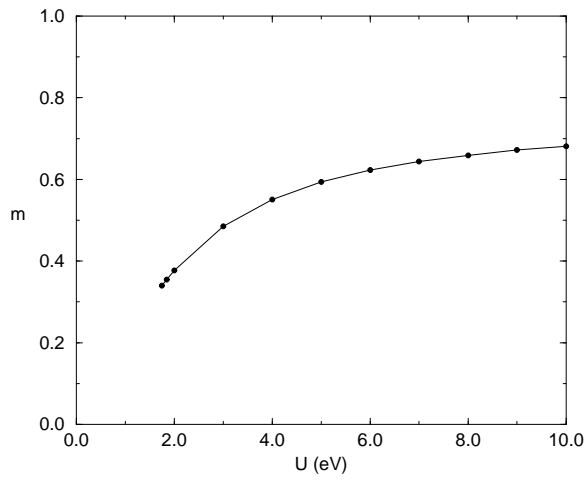


Figure 5

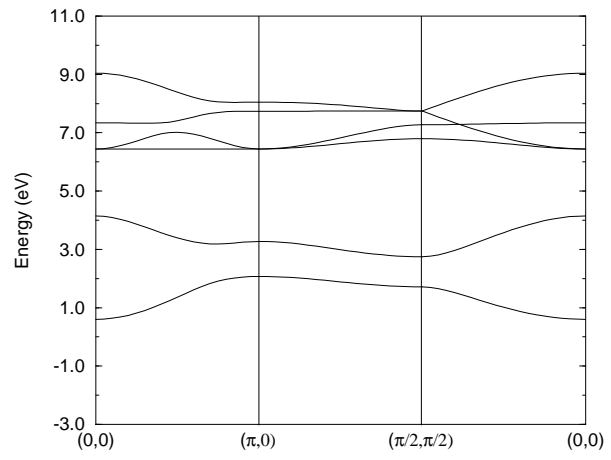


Figure 6

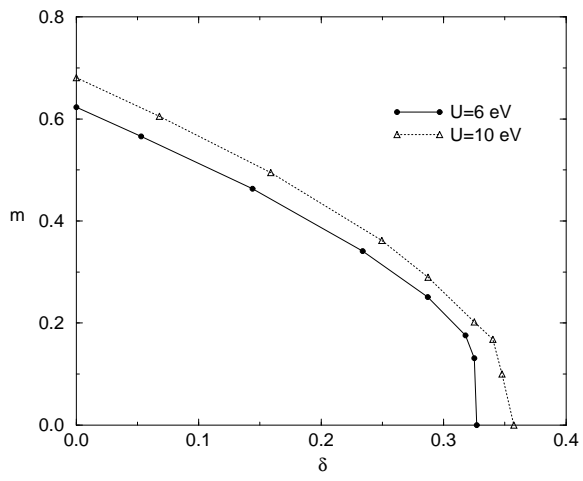


Figure 7

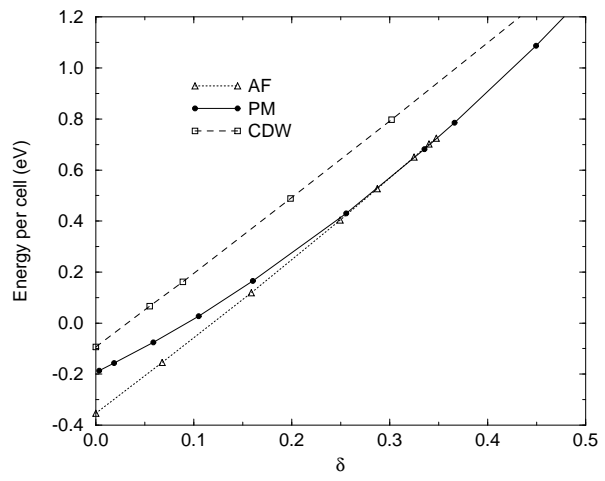


Figure 8

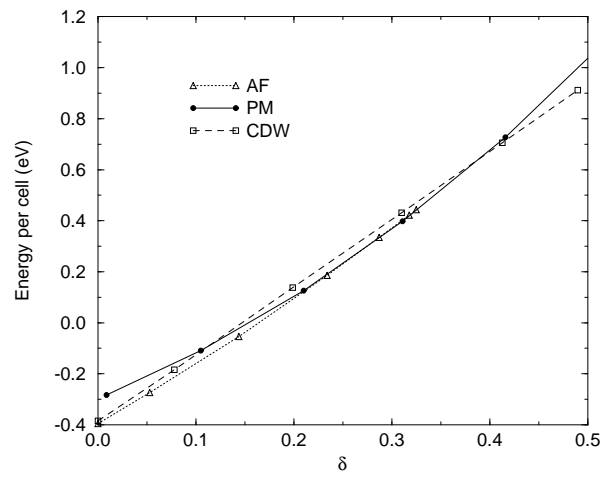


Figure 9